Fracture Mechanics of Concrete Structures,
Proceedings FRAMCOS-2, edited by Folker H. Wittmann,
AEDIFICATIO Publishers, D-79104 Freiburg (1995)

WATER MOVEMENT WITHIN MORTAR ANALYZED AS A CAPILLARY FLOW

H. Akita
Department of Civil Engineering, Tohoku Institute of Technology, Sendai, Japan
T. Fujiwara
Department of Civil Engineering, Iwate University, Morioka, Japan

Abstract

In order to evaluate shrinkage stress and it's influence on fracture, it is necessary to predict water movement within concrete precisely. The non-linear diffusion equation has been successfully applied to water movement but only during the drying process. As a model which can be applied to both drying and wetting processes, capillary flow is considered to be worth examining as one possibility in order to establish a universal model. In the first step, one-dimensional water movement within mortar was studied both analytically and experimentally. A model consisting of capillaries with various sizes was adopted and water movement was analyzed by assuming that it was caused by capillary action. A good correlation was obtained between numerical results and experimental data.

1 Introduction

In FRAMCOS-1, the authors reported the behavior of shrinkage cracks in concrete analyzed using a fictitious crack model. For the analysis, it is necessary to predict water movement within concrete precisely in order to evaluate shrinkage stress. The non-linear diffusion equation

has been successfully applied to water movement but only during the drying process. As shown by Akita et al., the diffusion equation can not be directly applied to water absorption. From their results, the reason for this is that the coefficient of diffusion needs to be varied not only with water content but also with the distance from the absorption surface to the wetting front. A model is required which can be applied to both of these process, because drying and wetting processes are usual conditions for real concrete structures.

Capillary flow is considered to be worth examining as one possibility in order to establish such a universal model. In order to investigate this possibility, one-dimensional water movement within mortar was studied both analytically and experimentally. Initially, pore distribution in mortar was assumed to be expressed as a simple function of pore diameter. Then, a model consisting of capillaries with various sizes was derived from the pore distribution and water movement was analyzed by assuming that it was caused by capillary action. Capillary interaction was also taken into account by modeling it as a lateral flow between thin capillaries and thick ones.

2 Experiment

For the mix proportion of the mortar used in the specimens, water cement ratio was 53% and volumetric aggregate ratio was 53%. The specimens were made of high early strength Portland cement and were cured 7 days. Two basic states were examined as follows:

(1) Absorption from the oven dried state: in a 105 °C oven for one week.
(2) Drying from the saturated state after 7 days curing in water.

The specimens were 4×4×16 cm rectangular prisms. As illustrated in Fig.1, the four 4×16 cm faces were sealed by plastic film and paraffin in order to realize one-dimensional water movement. In addition, one of the two 4×4 cm faces was also sealed for the drying study (2).

The absorption specimens stood in water, allowing water to penetrate vertically from the 4×4 cm faces. The other 4×4 cm faces were exposed to the atmosphere at 20 °C and 60% relative humidity. The drying specimens were also exposed to the same atmosphere, but placed horizontally.

The specimens were split into nine or ten pieces as shown in Fig.1, and the water content was obtained from the weight difference before and after oven drying.

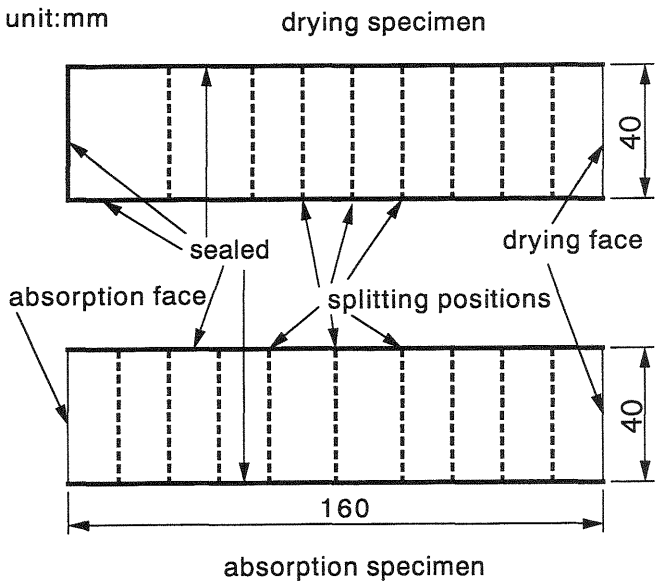

Fig. 1. Specimens

3 Analytical model

For the present analysis, the following assumptions were adopted.

3.1 Pore distribution

The pore distribution function ϕ of mortar was assumed to be expressed by the following equation

$$\phi = ar^{0.8}\exp\left(-br^{0.8}\right) + cr^{0.8}\exp\left(-dr^{0.8}\right) \tag{1}$$

where r is pore radius and a, b, c and d are constants which are shown in Table 1. The profiles of this function and the cumulative distribution function ψ are illustrated in Figure 2. The pore distribution was first experimentally determined by Uchikawa et al., and the expression for eq.(1) was first proposed by Shimomura et al.

3.2 Straight capillary model

Every pore of radius r was assumed to be modeled by straight capillaries of constant circular cross sections, also of radius r. The alignment of pores is actually not linear, but this discrepancy was considered by a shape factor to be mentioned later. The capillary distribution against r also coincides to eq.(1), because the total volume of capillaries of arbitrary r equals the total pore volume of the same

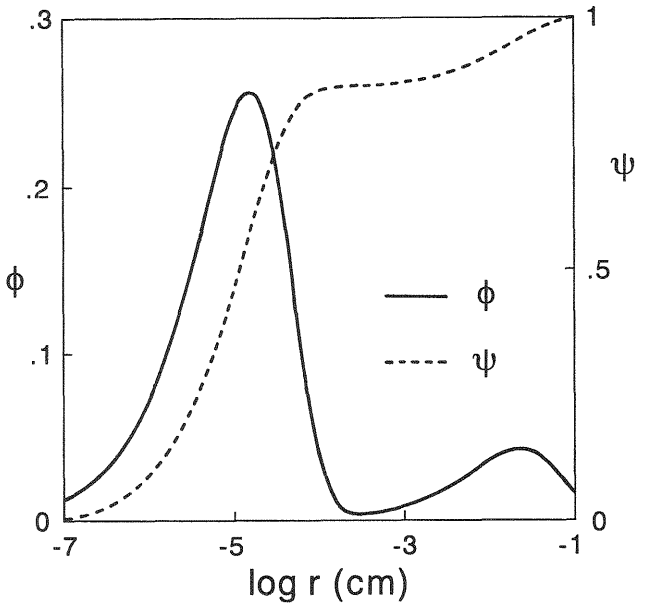

Fig. 2. Pore distribution function

Table 1. Constants in eq.(1)

a	614
b	7000
c	0.292
d	20

radius r. In the analysis, the continuous variation of r over the range shown in Fig.2 was modeled using discrete values r_i where i varies from 1 to 25.

3.3 Capillary rise equation

Capillary rise equation is derived from Hagen-Poiseuille's law as following:

$$v_i = \frac{2r_i\sigma\cos\theta}{G\mu(x_i + r_i)} - \frac{\rho g r_i^2}{G\mu} \qquad (2)$$

where x_i is the distance from the water surface to meniscus for each capillary i, v_i is the velocity of the meniscus, g is acceleration of gravity, G is the shape factor mentioned in the previous section, and σ, θ, ρ and μ are surface tension, contact angle, density and viscosity of water respectively. In order to avoid zero in the denominator, x_i was replaced by (x_i+r_i) in eq.(2) . It is correlated to the assumption that the water of a length r_i below the capillary entrance has the same velocity as the water in the capillary of radius r_i.

3.4 Capillary interaction

In the present analysis, the interaction among capillaries of different r was taken into account. This interaction produced a lateral flow because relatively thin capillaries pull water from thicker capillaries.

Considering that the lateral velocity is always zero both before and after flow laterally, the lateral velocity v_{ij} is derived as following from the motion equation for the case that an arbitrary capillary i pulls water from other capillary j

$$v_{ij} = 2\sigma\cos\theta\left(\frac{1}{r_i}-\frac{1}{r_j}\right)\left\{G'\rho x_{ij}\left(\frac{\mu}{\rho r_i^{\,2}}+\frac{2}{\Delta t}\right)\right\}^{-1} \tag{3}$$

where G' is the shape factor for lateral flow. It was assumed that the lateral flow occurred through lateral capillaries of radius r_i and the distance x_{ij} was

$$x_{ij} = x_i - x_j + 10r_i \tag{4}$$

where $10r_i$ was average distance between both capillaries.

3.5 Vapor diffusion

Vapor diffusion from each meniscus was also taken into account. The assumptions adopted were as follows.

The relative humidity in front of each meniscus was 100%, and diffusion occurs between the meniscus and the surface of the boundary layer at the drying face. The diffusion flux q_i is determined as follows;

$$q_i = D\frac{100-H_0}{G(L-x_i)+0.3} \tag{5}$$

where D is the diffusivity of vapor, H_0 is the atmospheric relative humidity, L is the specimen length and 0.3 cm is assumed as the thickness of boundary layer at the drying face.

3.6 Initial and boundary conditions

The initial condition for drying from the saturated state is

$$x_i = L \tag{6}$$

for all i, and that for absorption from the oven dried state is

$$x_i = 0 \tag{7}$$

The boundary condition is simply

$$0 \le x_i \le L \tag{8}$$

for both cases. However, a more detailed formula is necessary in order to perform the actual analysis. For example, the boundary condition for the drying surface is satisfied when

$$q_i\phi_i = \sum_{j=i+1}^{n} f_i v_{ij}\phi_i - \sum_{j=1}^{i-1} f_j v_{ji}\phi_j \qquad (9)$$

where f_i is the factor against maximum cosθ, considering that θ varies from 90° to 79°. It means that each meniscus is initially flat (fi=0) and f_i gradually increases, pulling water from other capillaries to cancel the loss by evaporation. After f_i reaches to unity, the meniscus begins to recede from the drying surface.

3.7 Material constants

The material constants in Table 2 can be found in data books of physical constants. Although the constants in Table 3 are assumed ones, they are values that are usually used in the analysis of water movement in soil. The value of the shape factor G' introduced in this study was selected so as to correlate the analytical results to the experimental ones.

3.8 Successive integration

Crank-Nicolson method was adopted as a successive integration method. Time intervals were initially 1 sec. incrementing by 1 sec. every 120 steps in the analysis of the drying process. On the other hand, they were

Table 2. Material constants

Surface tension of water	σ	7.275×10^{-6} N/m
Viscosity of water	μ	1.01×10^{-3} N·s/m
Diffusivity of vapor	D	2.49×10^{-5} m^2/s
Saturated vapor density		1.731×10^{-2} kg/m^3

Table 3. Other constants

Shape factor	G	130
Contact angle	θ	79°
Shape factor	G'	39000

initially 0.01 secs. incrementing by 0.01 secs. every 200 steps in that of the absorption process. These time intervals are far smaller than those used in the integration of the diffusion equation.

4 Numerical and experimental results

Figure 3 shows the profiles of relative water content for drying from the saturated state obtained from experiment and analysis. It can be seen that they both correlate well to each other. Figure 4 is a schematic illustration of the position of each meniscus in each capillary. The difference between these two figures is only that the capillary distribution function ϕ (Fig. 1) has been used as a weighting factor in Figure 3. It can be seen in both figures that pore distribution affects the water content profiles and meniscus distributions.

Figure 5 shows the same profiles for water absorption from the oven dried state. Fairly good correlation of both results can be seen except at lower values of water content. It can be seen that a small amount of water quickly rose into the specimen during the experiment. However, the wetting front is almost flat in the analytical result. The reason is considered that thin capillaries pull sufficient water from thick capillaries in the analysis. However, it should be mentioned that the velocities calculated by eq.(2) are smaller in thinner capillaries because of large friction forces.

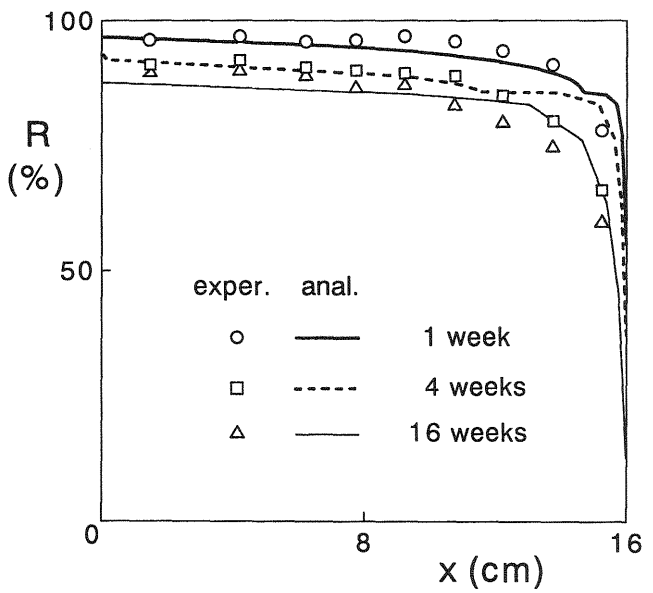

Fig. 3. Water content profiles for drying

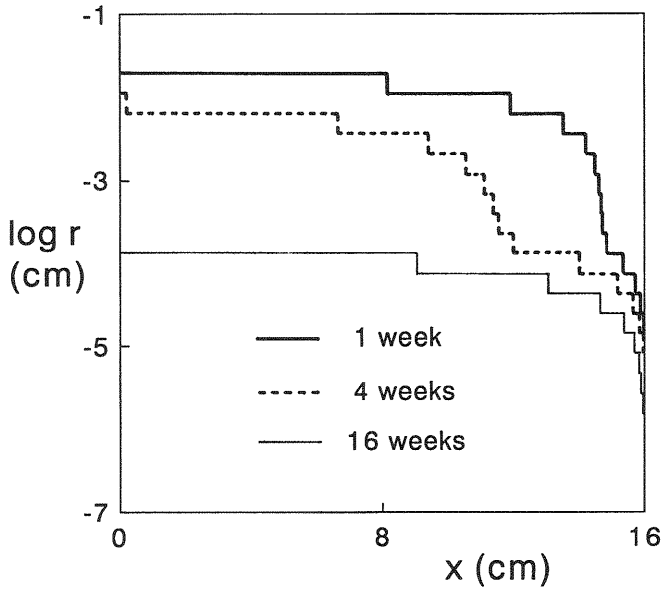

Fig. 4. Positions of meniscus

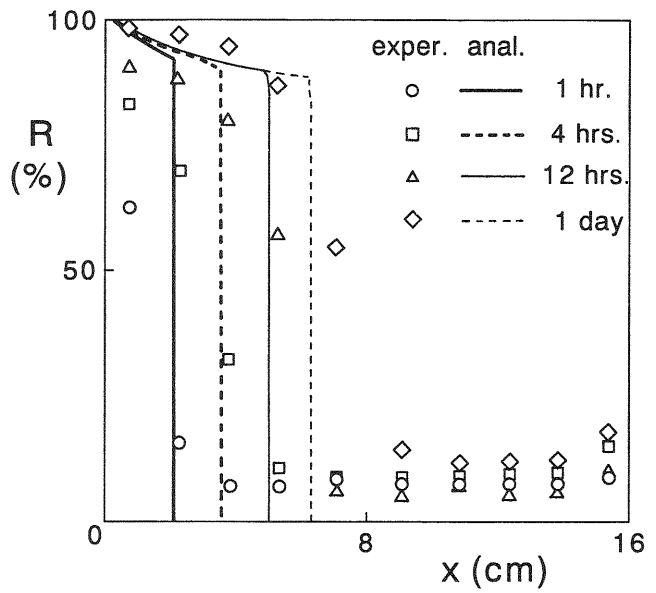

Fig. 5. Water content profiles for absorption

5 Conclusion

The following conclusions were derived from this study.

1. The analysis assuming a capillary flow is basically adequate to predict water movement within mortar.
2. It can be seen that pore distribution affects the water content profiles in the analysis of the drying process.
3. Compared with an analysis using the diffusion equation, far smaller time intervals in successive integration must be adopted in this method.
4. Further investigation might be necessary, because the present method does not give such good results for water absorption from the oven dried state in which capillary action seems the dominant process.

6 References

Akita, H., Fujiwara, T. and Ozaka, Y. (1992) Analysis of shrinkage cracks in concrete by fictitious crack model, in **Fracture Mechanics of Concrete Structures** (ed Z. P. Bazant), Elsevier, London, 967-970.

Akita, H., Fujiwara, T. and Ozaka, Y. (1990) Water movement within mortar due to drying and wetting. **Proc. JSCE**, No.420, 61-69.

Bazant, Z. P. and Najjar, L. J. (1972) Nonlinear water diffusion in nonsaturated concrete. **Materials and Structures**, 5, No.25, 3-20.

Kumar, S. and Malik, R. S. (1990) Verification of quick capillary rise approach for determining pore geometrical characteristics in soils of varying texture. **Soil Science**, 150, No.6, 883-888.

Sakata, K. and Kuramoto, O. (1981) A study on the water diffusion and shrinkage in concrete by drying. **Proc. JSCE**, No.316, 145-152.

Shimomura, T. and Ozawa, K. (1992) Water movement within concrete derived from assumed pore model. **Proc. JCI, 14**, No.1, 631-636.

Wittmann, F. H., Roelfstra, P. E. and Kamp, C. L. (1988) Drying of concrete: An application of the 3L-approach. **Nuclear Eng. and Design**, 105, 185-198.